

Spatial and temporal trends in carbonaceous aerosols in the United Kingdom

Jafar, Hanan A.; Harrison, Roy M.

DOI:

[10.1016/j.apr.2020.09.009](https://doi.org/10.1016/j.apr.2020.09.009)

License:

Creative Commons: Attribution-NonCommercial-NoDerivs (CC BY-NC-ND)

Document Version

Peer reviewed version

Citation for published version (Harvard):

Jafar, HA & Harrison, RM 2021, 'Spatial and temporal trends in carbonaceous aerosols in the United Kingdom', *Atmospheric Pollution Research*, vol. 12, no. 1, pp. 295-305. <https://doi.org/10.1016/j.apr.2020.09.009>

[Link to publication on Research at Birmingham portal](#)

General rights

Unless a licence is specified above, all rights (including copyright and moral rights) in this document are retained by the authors and/or the copyright holders. The express permission of the copyright holder must be obtained for any use of this material other than for purposes permitted by law.

- Users may freely distribute the URL that is used to identify this publication.
- Users may download and/or print one copy of the publication from the University of Birmingham research portal for the purpose of private study or non-commercial research.
- User may use extracts from the document in line with the concept of 'fair dealing' under the Copyright, Designs and Patents Act 1988 (?)
- Users may not further distribute the material nor use it for the purposes of commercial gain.

Where a licence is displayed above, please note the terms and conditions of the licence govern your use of this document.

When citing, please reference the published version.

Take down policy

While the University of Birmingham exercises care and attention in making items available there are rare occasions when an item has been uploaded in error or has been deemed to be commercially or otherwise sensitive.

If you believe that this is the case for this document, please contact UBIRA@lists.bham.ac.uk providing details and we will remove access to the work immediately and investigate.

1
2
3 **Spatial and Temporal Trends in Carbonaceous Aerosols**
4 **in the United Kingdom**
5

6 **Hanan A. Jafar^{1,2} and Roy M. Harrison^{3*†}**

7
8 (r.m.harrison@bham.ac.uk; hanan.a.jafar@gmail.com)
9

10
11 **¹Water and Environmental Studies Institute, An-Najah National**
12 **University, P.O. Box 7, Nablus, Palestine**

13
14 **²Civil Engineering Department, An-Najah National University**
15 **P.O. Box 7, Nablus, Palestine**

16
17 **³Division of Environmental Health & Risk Management**
18 **School of Geography, Earth & Environmental Sciences**
19 **University of Birmingham, Birmingham B1 52TT**
20 **United Kingdom**
21

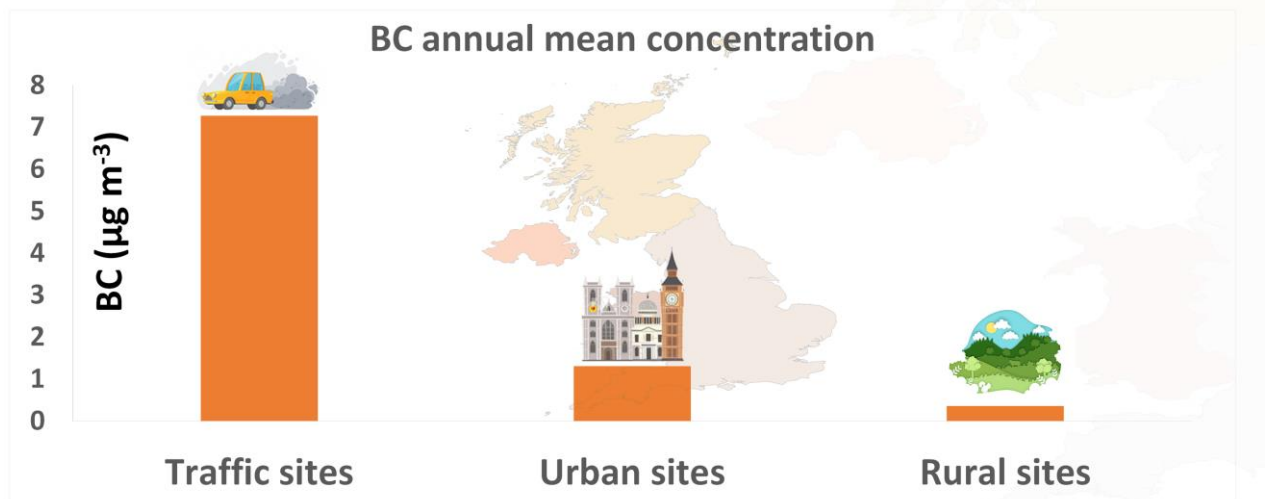
22
23 *Correspondence author: Roy M. Harrison, Division of Environmental Health and Risk
24 Management, School of Geography, Earth and Environmental Sciences, University of Birmingham
25 Edgbaston, Birmingham B15 2TT, United Kingdom. Email: r.m.harrison@bham.ac.uk
26 Tele: +44 121 414 3494; Fax: +44 121 414 3708;
27 ORCID ID: 0000-0002-2684-5226
28

29 †Also at: Department of Environmental Sciences / Center of Excellence in Environmental Studies,
30 King Abdulaziz University, PO Box 80203, Jeddah, 21589, Saudi Arabia
31

* To whom correspondence should be addressed.
Tele: +44 121 414 3494; Fax: +44 121 414 3708; Email: r.m.harrison@bham.ac.uk

† Also at: Department of Environmental Sciences / Center of Excellence in Environmental Studies, King Abdulaziz University, PO Box 80203, Jeddah, 21589, Saudi Arabia

32 **GRAPHICAL ABSTRACT:**
33



34 **Caption:** A substantial spatial gradient in black carbon is seen between traffic, urban background
35 and rural sites.
36
37
38

39 **ABSTRACT**

40 There is an increasing scientific interest in carbonaceous aerosols due to their effects on local air
41 quality and climate. The database of the UK air monitoring networks from 2009 to 2017 was
42 analysed to examine the trends in black carbon (BC), brown carbon (BrC), elemental carbon (EC)
43 and organic carbon (OC) at 11 sites with different classifications over the UK. The concentrations
44 increased from rural to urban background to kerbside sites. BC showed the strongest variation, with
45 maxima at kerbside ($> 9.0 \mu\text{g m}^{-3}$) and minima at rural sites (below $1.0 \mu\text{g m}^{-3}$). On the other hand,
46 BrC showed no clear variation according to site classification. BrC increased as domestic emissions
47 of wood smoke increased at weekends. Total OC and secondary OC showed a winter maximum at
48 urban and kerbside sites, while BC increased during the winter at urban sites and in autumn at
49 kerbside sites. Secondary Organic Carbon is dominated by regional transport processes. All
50 pollutants revealed a decreasing long-term trend in the UK, the most significant reduction was
51 observed in BC levels, particularly at the kerbside site ($-0.87 \mu\text{g m}^{-3} \text{yr}^{-1}$), with lesser rates of
52 decline (-0.08 to $-0.13 \mu\text{g m}^{-3} \text{yr}^{-1}$) at urban background sites. The general behaviour of BrC was
53 consistent with a major contribution from regional transport. As expected, EC shows similar
54 behaviour to BC, and OC/EC ratios have increased with time as diesel particle filters have reduced
55 EC emissions more than OC, and other sources of primary OC have not changed markedly.

56

57 **Keywords:** Elemental carbon; Organic carbon; Black Carbon; BrC; Emission trends;

58 Carbonaceous aerosols

59

60 1. INTRODUCTION

61 1.1 Overview

62 Carbonaceous aerosols (CAs) are ubiquitous in the atmosphere (Hand et al., 2013). The component
63 chemical species include Black Carbon (BC), Brown Carbon (BrC or UVPM; the two terms are
64 used interchangeably in this paper), Organic Carbon (OC) and Elemental Carbon (EC). Generally,
65 carbonaceous aerosols are accountable for 20%-50% of the total atmospheric Particulate Matter
66 (PM) mass (Contini et al., 2018). CAs contribute to the adverse health effects of particulate matter
67 exposure; reduce visibility and impact the atmosphere by scattering and absorbing solar radiation.
68 Thus, they contribute to climate forcing, which increases the scientific interest of these species
69 (Hand et al., 2013).

70

71 OC is a fraction of CAs that has light scattering properties, and thus has a cooling effect on climate
72 (Bahadur et al., 2012), it is typically 3–12 times higher than BC in mass in background air (Chen et
73 al., 2010). OC is considered a primary pollutant when it is emitted directly from incomplete
74 combustion of biomass and organic matter (Jones and Harrison, 2005). The emission factor from
75 combustion processes depends on combustion conditions and the type of fuel. Secondary organic
76 carbon (SOC) is formed in the atmosphere by gas to particle phase conversion of volatile organic
77 compounds (VOCs), which may be emitted from natural sources, burning of organic matter and
78 evaporation from fuel (Jones and Harrison, 2005). The key stage of SOC formation is the oxidation
79 of a VOC molecule to form a less volatile compound which then condenses (Hallquist et al., 2009).

80

81 Brown carbon is defined as the component of OC which absorbs light in the ultraviolet wavelength
82 region (Lack et al, 2014). BrC has both primary and secondary sources; it comprises emissions from
83 biomass burning, in the UK predominantly domestic wood burning, in addition to humic-like
84 substances arising from gas-phase oxidation of VOCs (Liu, et al., 2013; Chakrabarty et al., 2010).
85 BrC has a wide range of physicochemical properties that are difficult to be generalized (Andreae

86 and Gelencsér, 2006), and includes water-soluble and insoluble components. BrC (also referred to
87 as Delta-C in some studies) is often taken as representing wood-burning emissions, but this is often
88 not an accurate interpretation (Harrison et al., 2013).

89

90 The refractory light absorbing component of CAs is named BC or EC according to the
91 quantification method employed. The term EC is used when thermal optical methods are applied,
92 while BC is used when light absorption techniques are applied (Contini et al., 2018). When BC is
93 measured using an instrument such as an aethalometer it is called equivalent black carbon (eBC)
94 (Sharma et al., 2017). The term total carbon (TC) is defined as the sum of EC and OC measured by
95 thermal optical analysis (Petzold et al., 2013). BC and EC are emitted directly from incomplete
96 combustion processes, including on-road and off-road automotive sources (especially diesel
97 vehicles), domestic combustion of coal and public electricity power stations, in addition to waste
98 incineration and stationary combustion in manufacturing industries (Richmond et al., 2020).

99

100 These light-absorbing carbonaceous aerosols are driving forces for global warming (Andreae and
101 Gelencsér, 2006), and contribute to adverse health effects (WHO, 2012) and have high ability to
102 absorb and adsorb a range of toxic chemicals (Wang et al., 2014).

103 BC and EC have a relatively short lifetime in the atmosphere (between a few days to a few weeks)
104 compared to greenhouse gases (GHG), which have a much longer lifetime (ranges from several to
105 thousands of years). Therefore, any abatement strategies for BC and EC emissions will have a more
106 immediate effect on the regional scale to control climate change and reduce global warming (Chen
107 et al., 2012; Ramanathan and Carmichael, 2008).

108

109

110

111 **1.2 Trends in carbonaceous aerosols**

112 Several studies have investigated the spatial and temporal trends of CAs in Europe and worldwide
113 (Luoma et al., 2020; Zheng et al., 2020; Sun et al., 2020; Sommer et al. 2019; Kucbel et al., 2017;
114 Titos et al., 2017; Cavalli et al., 2016; Ahmed et al., 2014; Sandrini et al., 2014; Tiwari et al., 2013;
115 Querol et al., 2013; Backman et al., 2012; Sahu et al., 2011). CAs concentration was found to
116 increase significantly on moving from Scandinavia to Central Europe as a result of the atmospheric
117 pollution dilution (Cavalli et al., 2016). In Spain, maximum levels of eBC and BrC were observed
118 in Granada during a cold winter as a result of biomass burning, this influence was stronger in
119 suburban areas compared to the city centre (Titos et al., 2017). The same pattern was observed in
120 OC and EC concentrations in the Czech Republic by Mbengue et al. (2018) and at different urban
121 and rural locations across the Italian peninsula (Sandrini et al., 2014), whereas at rural sites in the
122 Northeastern United States, BC peaked in late summer (Ahmed et al., 2014).

123

124 Trends of BC over the UK have been investigated by Singh et al. (2018) over the period 2009–
125 2016; the analyses showed a decreasing trend in BC at 7 locations out of the 21 study locations. The
126 highest decrease in BC concentration was seen at Marylebone Road in London. Harrison and Yin
127 (2008) found that in the U.K. West Midlands, EC increased significantly on moving from rural to
128 urban to roadside sites, while the levels of OC at different sites showed a much smaller difference.
129 A chemical mass balance receptor model developed by Yin et al. (2010) detected the presence of
130 organic aerosols which were not related to primary sources and were attributed to secondary organic
131 aerosols (SOA).

132

133 Jones and Harrison (2005) reported that OC and EC did not show any systematic seasonal pattern
134 with one exception at the urban site of London North Kensington. It was clear that the non-traffic
135 sources of SOC and POC were predominant in the urban background at all times. At urban sites, the
136 concentrations of OC and EC were higher during weekdays compared to weekends (Jones and
137 Harrison, 2005). According to the analysis conducted by Charron et al. (2013), SOC could be

138 considered as regional pollutant. This is due to the uniformity shown by SOC across different sites
139 in the UK. The concentration field maps revealed that mainland European areas were important
140 sources for SOC at the study sites. Charron et al. (2013) emphasised the strong effect of air mass
141 back trajectories on EC levels at the rural Harwell site.

142

143 Most of published work and studies have focussed on one or two components of CAs, OC and EC
144 or BC in most cases. Moreover, a limited number of studies have been conducted in the UK related
145 to long-term temporal and spatial trends of different carbonaceous aerosols. Thus, this study aims to
146 investigate the long-term trends in CAs in the UK and examines seasonal, day of the week and
147 diurnal patterns for all metrics (BC, BrC, OC, SOC, POC and EC). A comparison of the
148 concentrations by site type is carried out and spatial patterns across the UK are investigated.
149 Finally, the long-term, seasonal and day of the week diurnal patterns in the traffic and urban
150 increments are examined.

151

152 **2. MATERIALS AND METHODS**

153 **2.1 Sampling and Analysis Methods**

154 Datasets from UK air monitoring networks for BC, BrC (UVPM), EC and OC were downloaded
155 from the UK-Air website (DEFRA, 2019) for use in this study. BC and BrC were monitored by the
156 Black Carbon Network, while OC and EC were monitored by the Particles Concentration Network.
157 Both monitoring networks are managed by the National Physical Laboratory and the Quality
158 Assurance protocols are provided in their reports (National Physical Laboratory, 2016a;b).

159

160 BC is measured using Magee scientific model AE22 aethalometers (Beccaceci et al, 2013). The
161 basic principle of this instrument is to measure absorption during transmission of light through a
162 sample collected on a filter tape. The aethalometers operate at two different wavelengths, 880 nm
163 and 370 nm. The first wavelength (880 nm) is used to quantify the concentration of BC, while the

164 second wavelength (370 nm) is used to measure BrC (Butterfield et al., 2016). The concentration of
165 the UV component is calculated by subtracting the concentration of BC measured at the 880 nm
166 wavelength from the concentration measured at 370 nm (Beccaceci et al, 2013).

167

168 The Thermo Partisol 2025 sequential air sampler is used for daily sampling of EC and OC PM₁₀
169 components (Beccaceci et al, 2013). The samples are collected on ultrapure quartz filters, and a
170 thermal/optical analyser is used to carry out the analysis of EC and OC based on the National
171 Institute for Occupational Safety and Health (NIOSH) protocol (PD CEN/TR 16243, 2011), where
172 the sample is heated first in a helium atmosphere to 870° C in order to remove OC, before it is
173 heated again up to 890° C in the presence of oxygen to detect EC (Beccaceci et al, 2013).

174

175 **2.2 Sampling Sites**

176 The number of BC Network sites has changed over the years (Butterfield et al., 2013). This has
177 created some gaps in the collected data and has limited the value of the data for comprehensive
178 analysis. For this study, and in order to achieve a high level of reliability, sites with the longest
179 measuring period and of significant importance were chosen. The start and end dates for the trend
180 analysis were not the same for all sites because they operated in different years.

181

182 The study focused on 11 sites in the BC and BrC monitoring network spread across different
183 regions of the UK. Regarding the EC and OC components of PM₁₀, the only monitoring sites in the
184 network are Harwell, London North Kensington and London Marylebone Road. Table 1 provides a
185 brief description of the study sites and lists the monitoring period for each site, and Figure 1 shows
186 the location of each site. Site details are available from (<https://uk-air.defra.gov.uk/>).

187

188

189 **2.3 Data Analysis**

190 The Open-air model was adopted through the different stages of this study to analyse the CA dataset.
191 One of Open-air's functions that was used in this study is the time variation function. This function
192 is used to find the diurnal, day of the week and monthly patterns in pollutant concentrations. It is
193 based on the 95% confidence interval, which is calculated by bootstrap re-sampling (Carslaw and
194 Ropkins, 2012). Another function is the PolarPlot function. This function plots the concentration of
195 pollutants on a polar coordinate, which is very useful to find the spatial distribution of pollutants
196 based on wind speed and direction (Carslaw and Ropkins, 2012). The TheilSen function was used for
197 long term trend analysis. This function uses the Mann-Kendall method with a linear regression in the
198 analysis process. The confidence interval for the TheilSen function is 95% (Carslaw and Ropkins,
199 2012). This method is insensitive to outliers and bootstrap-resampling is used to estimate the
200 parameters such as median (Agustine, 2017; Carslaw, 2015).

201 In order to compare EC and BC concentrations, the reduced major axis regression method (RMA)
202 was applied to the measurements (Garrett, 2018). RMA takes into consideration the uncertainty in
203 both x and y variables. In the case of pollutant concentrations, the error can occur in both x and y
204 directions because of uncertainty in measurements of both variables. Thus, RMA is preferable when
205 comparing EC and BC concentrations to least-squares regression which minimises the sum of squares
206 of the errors in the vertical direction (y) (Butterfield et al., 2016; Ayers, 2001).

207

208 For use in the EC tracer method to estimate the $(OC/EC)_{\min}$ ratio the scatterplot function was used,
209 where OC and EC concentrations (in $\mu\text{g m}^{-3}$) of a given year were used to produce the scatterplot
210 with OC on the y-axis and EC on the x-axis. Then the slope of the line which passes through the
211 origin and the lowest points was calculated. This slope represents $(OC/EC)_{\min}$ for that year (Pio et
212 al., 2011). Any points above this line indicate the formation of SOC. Then the daily values of POC
213 and SOC for each year were calculated according to the following equations:

$$214 \text{ POC} = (OC/EC)_{\min} \times EC + OC_{\text{non-combustion}} \quad (1)$$

215 $SOC = OC - POC$ (2)

216

217 where $(OC/EC)_{min}$ is the ratio of OC to EC from primary sources at the study area, $OC_{non-combustion}$ is
218 primary OC from non-combustion sources (Lin et al., 2009). In this study it was assumed that
219 $OC_{non-combustion}$ equals zero. This was conducted year by year as the composition of primary aerosol
220 and hence $(OC/EC)_{min}$ can change with time.

221

222 The urban increment was calculated by subtracting simultaneous measurements at Harwell (rural)
223 from North Kensington (urban background) data, while the roadside increment was calculated by
224 subtracting simultaneous measurements at North Kensington from Marylebone Road (roadside).

225

226 **3. RESULTS AND DISCUSSION**

227 **3.1 Time Variation Analysis**

228 The diurnal profile of BC at the roadside site of Marylebone Road followed the traffic flow over the
229 day. This is expected because the main source for BC in the European cities is incomplete fuel
230 combustion in automobiles, particularly diesel vehicles (Sommer et al., 2019). All days of the week
231 showed the same pattern where BC levels increased substantially between 6:00 and 18:00, but at
232 weekends the levels were lower compared to weekdays (Figure 2), as also observed by Singh et al.
233 (2018). This is attributed to a drop in traffic flow, especially in heavy diesel vehicle numbers during
234 weekends at Marylebone Road (Butterfield et al., 2016). Similar weekly cycles were observed at
235 traffic stations across Germany (Kutzner et al., 2018) and at traffic sites in Zurich and Bern,
236 Switzerland (Zotter et al., 2017; Reche et al., 2011). BC revealed weak seasonality dependence,
237 where the lowest concentrations (less than $6.5 \mu\text{g m}^{-3}$) were in spring and the highest (above $8.0 \mu\text{g}$
238 m^{-3}) were in autumn (Figure 3). This is unlikely to be due to changes in traffic emissions between
239 spring and autumn, but due to the change in the relative amounts of southerly and northerly winds

240 between the seasons, where northerly winds were dominant in spring; the effect of wind direction is
241 discussed in Section 3.3.

242

243 BrC revealed an opposite behaviour to BC at Marylebone Road, where the concentration decreased
244 to less than zero in daytime and increased at night (Figure S1). These negative concentrations were
245 observed by Harrison et al. (2013) at Marylebone Road and by Butterfield et al. (2016) at different
246 sites over the UK, especially roadside sites. The cause of these negative spikes might be the semi-
247 volatile organic species from vehicle-exhaust, which are collected on the filter and increase UV
248 absorption. These semi-volatile aromatic organic species may evaporate over time and cause
249 negative artefact concentrations of BrC at roadside sites in particular. The elevated BrC levels at
250 night during all days of the week are likely because of higher emissions from wood burning,
251 enhanced condensation of semi-volatile components, and more stable atmospheric conditions which
252 trap the pollutants due to less effective dispersion. BrC measurements during weekends were higher
253 than weekdays, and peaked in winter (Figure 3) due to residential heating and winter-time
254 inversions. This study is consistent with Titos et al. (2017) where BrC levels over Granada, Spain,
255 increased in winter. Similar seasonality as well was recorded at different sites over Europe by
256 Lukács et al. (2007).

257

258 At urban background sites, Birmingham Tyburn, North Kensington and Cardiff, the morning BC
259 peak was around 09:00 local time coinciding with the traffic morning rush hour (Figures S2, S3 and
260 S4). BC levels also increased during the evening due to a conjunction of heavy traffic and a
261 decrease in boundary layer depth. Elevated levels of BC were recorded on weekdays compared to
262 weekends, which reflects a traffic signature on BC profiles at these sites. The BrC component at the
263 three sites showed a slight increase in the morning and a rapid increase over the night (Figures S5,
264 S6 and S7), which could be related to a night-time inversion, secondary home heating and the
265 formation of secondary BrC due to night-time chemistry.

266 The urban sites in Northern Ireland revealed the same patterns in BC and BrC concentrations and
267 the two metrics had similar behavior (as illustrated in Figure S8, S9, S10) for BC, and Figures S11,
268 S12, S13 for BrC). A small peak due to morning rush-hour traffic was observed in the diurnal
269 profiles and the concentrations of BC and BrC increased at night to peak at around 20:00 at
270 Strabane and Ballymena, while the peak at Kilmakee was two hours later. The reason for this
271 increase is likely to be less effective mixing and dispersion at night, and residential heating, which
272 is predominantly by solid and liquid fossil fuel at Strabane and natural gas at Ballymena and
273 Kilmakee. No difference was noticed between BrC and BC measurements at weekdays and
274 weekends (except for the rush-hour effect which disappeared at weekends), because the dominant
275 source of BC at these sites is mainly domestic emissions which do not vary during the week as
276 traffic flow does.

277

278 At Belfast Urban Centre, the traffic-based signature was clearly seen due to elevated levels in BC
279 coinciding with the morning rush-hour, after which the concentration was fairly constant between
280 17:00-23:00 (Figure S14). BrC levels dropped in daytime and increased at night, which could be
281 because of residential heating and night-time atmospheric processes (Figure S15). On Saturday
282 evenings and Sunday early mornings, BC and BrC concentrations increased slightly, probably due
283 to traffic and biomass burning respectively. Apart from this, no difference was observed between
284 trends at weekends and weekdays.

285

286 BrC and BC revealed seasonal dependence at urban background sites and Belfast Urban Centre
287 (Figures S16, S17, S18, S19, S20, S21, S22). Both metrics showed elevated levels in winter and
288 low levels in summer. This is attributed to less effective atmospheric mixing in winter and higher
289 local emissions, particularly from domestic heating compared to summer, as is the case in other
290 European urban areas where biomass burning is a significant source for CAs (Kutzner et al., 2018;
291 Titos et al., 2017).

292 Similar diurnal, weekly and seasonal profiles of BC were observed in previous studies at urban and
293 sub-urban sites in the UK (Singh et al., 2018; Harrison et al., 2013), in urban sites across Germany
294 (Sun et al., 2020) and at urban areas in Barcelona and Granada, Spain (Viana et al., 2013; Titos et
295 al., 2017). The diurnal and seasonal profiles of BrC are consistent with Harrison et al. (2013) and
296 are in line with the maximum levels of BrC that were observed during Vienna and Granada cold
297 winters as a result of biomass burning, where the influence was stronger in suburban areas
298 compared to the city centre (Sommer et al., 2019; Titos et al., 2017).

299

300 At rural sites, the lowest BC levels were recorded compared to other study sites. However, a small
301 effect of the morning rush-hour was still evident (Figures S23, S24, S25). Due to this very weak
302 effect of traffic, BC levels showed a relatively flat weekly cycle. Both BC and BrC (Figures S26,
303 S27, S28) increased at night which could be due to a night-time inversion and shallower PBL,
304 beside stronger local wood burning emissions at night. Since BrC is not directly affected by traffic
305 (which has higher emissions at weekdays compared to weekends), the concentrations were fairly
306 constant over the week.

307

308 Most rural sites showed low levels of BrC in summer and high levels in winter (Figures S29, S30,
309 S31), which seems to be due to less effective mixing in winter and higher emissions from wood
310 burning for heating. However, BC concentrations at Detling and Auchencorth Moss revealed no
311 seasonal dependence, while Harwell showed very weak seasonality.

312

313 Regarding EC, OC, SOC and POC at Marylebone Road, these pollutant metrics decreased sharply
314 at weekends (Figures S32 and S33) due to reduced traffic flows on Sundays and Saturdays, which is
315 a major source for EC and POC at this site. EC revealed the same seasonal pattern as BC, as the two
316 pollutants are emitted from the same sources, but are operationally defined (Figure S34). OC in
317 general showed maxima in winter and minima in summer, the levels of SOC showed the same

318 trend, while POC displayed elevated levels in autumn and low levels in spring (Figure S35).
319 Moreover, the concentrations of SOC were higher than simultaneous concentrations of POC. The
320 low levels of SOC in summer may be attributable to semi-volatile SOA compounds which change
321 to the gaseous-phase at higher temperatures. The high levels in winter may be attributed to an
322 increase in anthropogenic precursor emissions and less effective dispersion compared to summer,
323 whereas, elevated POC concentrations in autumn and low levels in spring could be related to
324 changes in the relative amounts of southerly and northerly winds between the seasons rather than a
325 change in traffic emissions. It is important to remember that the graphical method used for
326 separating the two components of OC is far from perfect. It is likely that even at the lowest OC/EC
327 ratios, there is still some SOC, and there is no situation in the UK where there is no SOC (Jones and
328 Harrison, 2005). This is a flaw in the technique and there is no way of allowing for it.

329
330 London, North Kensington revealed a slight decrease in OC, SOC, POC and EC over weekends
331 (Figure S36 and S37), because it is an urban background site that is affected by traffic movement
332 through the week. EC, OC and POC revealed maxima in winter and minima in summer (Figure S38
333 and S39), which might be due to higher emissions and especially less effective mixing in winter.
334 However, SOC did not display any seasonality, one possible explanation is the SOA semi-volatile
335 nature, which causes some volatilisation at high summer temperatures, despite more effective
336 photochemical formation in summer. Another reason could be the increase in residential precursor
337 emissions in winter, mainly from heating and wood burning. The latter is known to oxidise rapidly
338 to SOA after emission. Concentrations at Harwell were fairly constant over the whole week (Figure
339 S40 and S41), because the site is dominated by sources other than traffic, such as the regional
340 background, and local domestic and biogenic emissions from surrounding sources. These emissions
341 do not vary over the week to the same extent as traffic flow. SOC was the only metric which
342 revealed seasonal dependence at this site (Figure S42 and S43), where maximum levels were
343 recorded in summer, which is consistent with Charron et al. (2013). This might be the result of high

344 biogenic precursor concentrations and photochemical activity which increase in the warmer months
345 and enhance the formation of SOC by gas-particle conversion. The same seasonal pattern was
346 observed in OC and EC concentration across Germany (Kutzner et al., 2018), the Czech Republic
347 (Mbengue et al., 2018), in Granada, Spain (Titos et al., 2017), and at different urban and rural
348 locations across the Italian peninsula (Sandrini et al., 2014).

349

350 A substantial spatial variation in BC, EC, OC, POC and SOC was clearly seen amongst the study
351 sites. The concentrations increased from rural to urban background to kerbside sites. BC showed the
352 strongest variation, The highest annual mean concentration of BC amongst the 12 sites was $7.28 \pm$
353 $2.32 \mu\text{g m}^{-3}$ at Marylebone Road, and the concentration decreased with respect to distance from BC
354 emission sources to reach minima at rural sites ($0.36 \pm 0.15 \mu\text{g m}^{-3}$), while the urban background
355 sites recorded an annual mean concentration of $1.31 \pm 0.25 \mu\text{g m}^{-3}$, which is in line with the Singh et
356 al. (2018) findings in the U.K.. Similar trends in BC variation have been reported across Europe; in
357 Finland, Germany and Italy (Luoma et al., 2020; Kutzner et al., 2018; Sandrini et al., 2014). The
358 annual mean concentrations of BC for traffic, urban background, and rural sites were close to those
359 reported by Kutzner et al. (2018) in Germany.

360

361 *Urban increment*

362 The urban increment is related to emission sources in the city. The urban increment of BC in
363 London, provides an evidence of the effect of commuter traffic movement on BC levels at North
364 Kensington, since the increment shows a peak coinciding with the morning rush-hour and a slight
365 drop at weekends as traffic flow decreased (Figure S44), while the increase in the increment at
366 night-time indicates the presence of domestic heating emissions. Since BrC is often taken as
367 representing wood-burning emissions, the increase in the urban increment of BrC at night (Figure
368 S45) emphasizes the presence of domestic heating emissions at night-time in North Kensington.
369 The EC increment shows the same behaviour as the BC increment (Figure S46), since they have the

370 same emission sources. Both increments increased in November and decreased from May to July
371 (Figure S47). The OC increment was fairly constant over the week (Figure S46), which means
372 traffic is not the dominant source of OC at North Kensington, and it increased in winter due to
373 higher residential heating emissions and fell in summer (Figure S48), which indicates the strong
374 effect of the heating season on OC levels in the London urban background just as at urban
375 background sites in Granada and Barcelona in Spain (Titos et al., 2017; Viana et al., 2013), Paris in
376 France (Weimer et al., 2009) and in Germany (Kutzner et al., 2018) where the effect of biomass
377 burning is evident on CA levels during the heating season.

378

379 *Roadside increment*

380 The roadside increment makes it easier to separate the changes in concentrations due to regional
381 processes (such as dynamics of PBL, meteorological conditions and regional emissions) from those
382 of local traffic emissions. The roadside increment in BC followed the expected profile of daily
383 traffic flow (Figure S49), where elevated levels were seen in the morning and evening rush-hours,
384 and low concentrations at weekends, which provides evidence of vehicle emissions as a major
385 source for BC at Marylebone Road similar to other traffic sites across Europe in Finland, France,
386 Austria, Germany, Switzerland and Italy (Luoma et al., 2020; Font et al., 2019; Sommer et al.,
387 2019; Kutzner et al., 2018; Zotter et al., 2017; Sandrini et al., 2014; Reche et al., 2011). The diurnal
388 and day of the week profiles of roadside increment of BrC were clearly affected by the negative
389 concentrations of BrC observed at Marylebone Road (Figure S50). The EC roadside increment
390 showed the same pattern as the BC increment due to similar sources (Figure S51). The EC and BC
391 traffic-related increment displayed elevated levels from July to October and minima in spring
392 (Figure S52), for which the possible explanation is a change in the relative amounts of southerly
393 and northerly winds between the seasons at Marylebone Road (Figure S53), which is discussed in
394 Section 3.3. The roadside increments in OC at weekends were lower than weekdays (Figure S51),
395 due to drop in the vehicle fleet size on Sundays and Saturdays. Moreover, the OC increment

396 revealed no clear seasonal dependence, but increments in autumn and winter were generally higher
397 compared to spring and summer (Figure S54). This emphasizes the effect of other factors besides
398 traffic emissions on OC levels at Marylebone Road, such as domestic heating. The roadside
399 increment of EC/OC ratio in London was higher than 1.0 on all days of the week (Figure S55)
400 which suggests that in vehicle emissions at Marylebone Road, the levels of EC exceed OC, whereas
401 at rural and urban background sites OC is typically predominant. All months except November
402 showed a roadside increment ratio of EC/OC higher than 1.0 (Figure S56). The low increment ratio
403 in November (about 0.8), is due to a slight drop in EC roadside increment coinciding with an
404 increase in OC increment during that month.

405

406 **3.2 Long Term Trend Analysis**

407 The largest decrease in BC levels over the period 2009-2017 was recorded at Marylebone Road
408 ($-0.87 \mu\text{g m}^{-3}/\text{year}$, Figure 4). This significant reduction is attributed to effective policies and
409 standards for vehicle exhaust emissions, and implementation of low emission zones, besides
410 promotion of walking and cycling. The reduction in roadside increment of BC in London
411 strengthens this explanation (Figure S57 (A)). The findings of Singh et al. (2018) emphasise the
412 effect of traffic-emissions abatement policies to reduce BC levels significantly in London as
413 suggested by the current study. The urban background sites showed a downward trend in BC ranged
414 between -0.08 and $-0.13 \mu\text{g m}^{-3}/\text{year}$ (Figures S58, S59, S60, S61, S62), except for Strabane where
415 the decreasing trend was not significant. The levels at rural sites revealed a lower decrease in BC
416 compared to kerbside and urban background sites (Figure S63). This could be attributed to the
417 sources of BC that are dominant at each site, for example at the kerbside site the main source is
418 traffic, thus any restriction on vehicle emissions will directly reduce BC levels. Urban background
419 sites are still affected by traffic emissions beside the local and regional sources, so the effect of
420 vehicle emissions control is still evident at these sites, but rural sites are the least affected by traffic

421 emissions and more influenced by the regional background, which declines more slowly over the
422 years.

423

424 In the broader context, decreasing trends in BC mass concentration were also reported at different
425 sites in Germany, Austria and Finland (Luoma et al., 2020; Sun et al., 2020; Sommer et al., 2019;
426 Kutzner et al. 2018). The highest decrease was at traffic sites which is most likely due to the efforts
427 of the European Union to mitigate anthropogenic emission through various policies and programmes
428 (Luoma et al., 2020; Sommer et al., 2019; Sun et al., 2020), especially the requirement for diesel
429 particle filters on new vehicles.

430

431 The BrC component at Marylebone Road revealed an upward trend ($+ 0.04 \mu\text{g m}^{-3}/\text{year}$, Figure 4)
432 over the study period. This increase seems likely to be due to local residential emissions of wood
433 smoke, since the levels of both BC and BrC dropped slightly at North Kensington (Figure S58 (B)),
434 which is affected by domestic emissions more than traffic relative to Marylebone Road. Moreover,
435 looking on the trends in urban and roadside increments of different metrics in London, the roadside
436 increment of EC, BC and OC decreased (Figure S57), while the urban increment was fairly constant
437 over time (Figure S64). All urban background sites showed a downward trend in BrC levels, but
438 this change was not significant, except at Birmingham Tyburn and Ballymena (Figures S58 (A) and
439 S60), probably due to a reduction in local wood smoke emissions, whereas the levels at rural sites
440 were fairly constant over the study period, which provides strong evidence of long-range transport
441 of BrC which is in line with Viana et al. (2013) where the source apportionment analysis showed
442 evidence of the contribution of regional transported SOA and biomass burning contributors to the
443 CA load at a rural site in Barcelona, Spain, and agrees with what has been reported in a rural area in
444 the Czech Republic, where the high pollution episodes of CAs were mainly associated with
445 continental air masses (Mbengue et al., 2018).

446 The concentration of total OC at Marylebone Road dropped ($-0.3 \mu\text{g m}^{-3}/\text{year}$, Figure S65 (A)) over
447 the period 2009-2017. This decrease is mainly due to reduction in the estimated SOC component ($-$
448 $0.27 \mu\text{g m}^{-3}/\text{year}$, Figure S66 (A)). A downward trend in the OC roadside increment was also
449 observed (Figure S57). The same trend was revealed at North Kensington, but the reduction was
450 smaller ($-0.15 \mu\text{g m}^{-3}/\text{year}$ in OC and $-0.1 \mu\text{g m}^{-3}/\text{year}$ in SOC, Figures S65 and S66, respectively),
451 due to a larger influence of other local sources than traffic. A downward trend was also seen at
452 Harwell, but the trend was not significant, emphasizing the contribution of the regional background.
453 However, POC downward trends at the three sites were not significant (Figure S66), which suggests
454 fairly constant regional emissions over the study period as reported by Sun et al. (2020) who
455 analyzed the German Ultrafine Aerosol Network over the period 2009-2018.
456 EC revealed the same temporal and spatial trends as BC, but the downward trends of EC were
457 always smaller (Figure S65). As shown in Section 3.4, the relationship between BC and EC was
458 site-dependent probably reflecting some source-dependency of BC/EC ratios. This would lead to
459 differing spatial and temporal trends as the relative source contributions to BC and EC change with
460 time. The significant reduction in EC at Marylebone Road is directly reflected in the EC/OC ratio
461 (Figure S67), where the ratio decreased by $-0.04 /\text{year}$. The EC/OC ratio at North Kensington and
462 Harwell was fairly constant, due to the slight decrease in both EC and OC at North Kensington and
463 fairly constant concentrations of EC and OC at Harwell over the study period.

464

465 **3.3 Effect of Wind Direction on Concentration**

466 Atmospheric concentration of primary and secondary pollutants can be greatly affected by wind
467 speed and direction. Marylebone Road is different from other sites, it is a street canyon (an urban
468 street, which is surrounded by high buildings on both sides) with an aspect ratio about 0.8 (mean
469 height of buildings to width of street ratio). These characteristics significantly affect the dispersion
470 of pollutants within the street canyon, due to recirculation of air and formation of a vortex that traps
471 the pollutants in the leeward direction inside the canyon in the case of perpendicular wind-flow

472 (Nataraj et al., 2020; Jones and Harrison, 2005). The road is aligned 255° to 75° (approximately
473 west-east direction) and the monitoring station is to the south of Marylebone Road, which makes it
474 in the leeward direction when the wind above the canyon is from the south. Thus, southerly winds
475 are expected to have the greatest enhancement of pollutant concentrations at Marylebone Road
476 (Jones and Harrison, 2005).

477

478 The concentrations of BC, EC and POC at Marylebone Road were enhanced by south and southwest
479 winds (Figures 5, S68 and S69). The BrC component showed the highest levels with easterly and
480 westerly winds. SOC levels increased with southeasterly winds and the concentration of total OC
481 showed a maximum in southerly and near southerly winds, while the lowest levels of all pollutants
482 were observed with northerly winds. These results emphasize the effect of southerly wind
483 perpendicular to the road in enhancing the concentrations of those pollutants emitted at Marylebone
484 Road, due to the location of the monitoring station on the leeward side, as seen in other studies at this
485 site. Northerly winds have the least effect, because in this case the monitoring station is on the
486 windward side and the canyon is filled with background air from north London. The effect of parallel
487 winds (easterly and westerly) is also obvious in increasing the concentrations of BC, EC and POC.
488 As BrC is not an emission within the canyon, it would be expected to show a different directional
489 dependency, more related to local woodsmoke sources.

490

491 At North Kensington, the concentrations of all pollutants revealed no dependence on wind direction
492 except for east and south-east winds (Figures S70, S71 and S72). This indicates a combination of
493 local emissions and transport of aged air masses from central London (which is located to the south-
494 east of North Kensington) and the European mainland. SOC was the pollutant which was most
495 enhanced by easterly and south-easterly winds due to the contribution of regional transported SOA

496 from continental air masses. The influence of these air masses on CAs concentration has also been
497 observed in Barcelona, Spain (Viana et al., 2013).

498
499 BC and BrC concentrations at Birmingham Tyburn and Belfast did not reveal a significant
500 dependence on wind direction (Figures S73 and S74), which implies that the predominant source of
501 BC and BrC at these sites is local emissions from all directions. At Cardiff, the concentration of
502 BrC and BC increased with easterly and near easterly winds (Figure S75), which could be
503 attributable to aged air masses from London and mainland Europe affecting the site. At Ballymena,
504 BC did not reveal a variation with wind direction (Figure S76), which suggest local emissions as the
505 main source for BC, while BrC was enhanced by westerly wind, which might be due to regional
506 pollutant transport.

507

508 At the Harwell rural site, all pollutants were enhanced by easterly and south easterly winds (Figures
509 S77, S78 and S79), which could be attributable to the emissions from the major A34 highway at a
510 distance of 1.85 km from the station, and air masses from London and the European mainland. The
511 levels of BC at Auchencorth Moss were enhanced by southeasterly winds, and BrC levels increased
512 with easterly winds (Figure S80), which is attributed to a possible effect of the A701 road and regional
513 transport of pollutants. At Detling, southeasterly and easterly winds enhance the concentrations of
514 BC and BrC (Figure 6), which seems likely to be due to regional transport of air masses from
515 mainland Europe.

516

517 **3.4 Relationship Between BC and EC**

518 Hourly concentrations of BC were measured by the Black Carbon Network, while daily
519 concentrations of EC were measured by the Particles Concentration Network. BC measurements at
520 Marylebone Road, North Kensington and Harwell were converted to daily averages and plotted

521 against the corresponding EC measurements for the whole study period (2010-2017 at Marylebone
522 Road and North Kensington, 2010-2015 at Harwell). There was a good correlation ($R^2 > 0.7$)
523 between BC and EC at the three sites (Figure 7). The value of R^2 was highest at Marylebone Road
524 ($R^2 = 0.88$), followed by North Kensington ($R^2 = 0.79$) and Harwell ($R^2 = 0.74$). The intercepts at
525 the three sites were relatively small (less than 0.13), and the gradients were respectively 0.70, 0.74
526 and 0.62.

527

528 BC and EC are essentially the same component, but are operationally defined by their measurement
529 procedures, where BC is measured by optical absorption, and EC by combustion. BC is measured
530 by aethalometer, which uses a mass absorption coefficient of $16.6 \text{ m}^2 \text{ g}^{-1}$ (that is recommended by
531 the manufacturer) to convert the light absorption to BC concentration. According to the regression
532 results, the aethalometer over-estimates BC levels relative to EC, as was also reported by Merico et
533 al. (2019). Similar results were observed by Chang et al. (2017) between collocated aethalometer
534 BC and Sunset Laboratory EC concentrations in Shanghai, China, in all seasons over the period
535 2009-2014. Also, Merico et al. (2019), working at a Mediterranean site found a measurement
536 protocol-dependence of EC measurements, and a seasonal dependence of OC/EC ratios which may
537 be related to differing ratios of brown to black carbon between the seasons which can influence both
538 optical and thermal measurements in different ways.

539

540 **3.5 OC/ EC Minimum Ratio**

541 The estimation of $(\text{OC}/\text{EC})_{\min}$ at Marylebone Road, North Kensington and Harwell has been
542 described above, and is illustrated in the Supplementary Information (Figures S81 to S83), where
543 scatter plots using the measurements of OC and EC for one year of daily data are presented.

544

545 $(\text{OC}/\text{EC})_{\min}$ increased significantly from Marylebone Road to North Kensington to Harwell (Table
546 2) which emphasize the effect of urban traffic as a main driver of EC emissions at roadside sites and

547 reflects the importance of regional emissions and atmospheric transport on OC concentrations at
548 rural sites. This tendency and similar results have been observed in previous studies in Europe and
549 the UK (Sandrini et al., 2014; Pio et al., 2011; Yin et al., 2010; Yin and Harrison, 2008) despite the
550 difference in measurement and analysis techniques.

551

552 The ratio of $(OC/EC)_{min}$ revealed an increasing trend at Marylebone Road, North Kensington and
553 Harwell over the period 2009-2017 (Figure S84), although the trends were not significant. The
554 $(OC/EC)_{min}$ ratios observed at Marylebone Road (Table 2) are expected to reflect the emissions
555 from road vehicles. The ratios for 2010 – 2012, with a mean ratio = 0.42 are reflective of emissions
556 from diesel engines prior to the mandatory fitting of diesel particle filters (DPF), and are consistent
557 with data derived from a measurement campaign in the UK West Midlands conurbation which
558 reported a typical value of 0.40 (Harrison and Yin, 2008). The data then show a steady increase in
559 $(OC/EC)_{min}$ as the emissions from gasoline engines with a higher particulate OC/EC ratio have
560 become more prominent.

561

562 **4. CONCLUSION AND RECOMMENDATIONS**

563 The dataset was insufficient to define a detailed spatial distribution. However, the concentrations of
564 pollutants showed a marked variation between sites with different characteristics. BC revealed the
565 strongest variation, the highest levels were at Marylebone Road, while the lowest were at rural sites.
566 This is directly related to the large effect of vehicle exhaust emissions at Marylebone Road
567 compared to the other study sites. A weak spatial variation was seen in the BrC component, with the
568 levels at Northern Ireland urban sites higher than other background sites and rural sites, presumably
569 due to greater use of biomass fuels. EC, OC, SOC and POC showed the same tendency as BC
570 indicating a strong influence of anthropogenic emissions. However, $(OC/EC)_{min}$ ratio increased as
571 traffic emissions became less dominant to reach maxima at rural sites (2.7 ± 0.6).

572

573 The traffic signature was still obvious at urban background and rural sites as well as at the kerbside
574 site, where the concentration of BC showed a peak coinciding with the morning rush hour. At
575 Marylebone Road all pollutants except for BrC showed lower levels at weekends compared to
576 weekdays, reflecting traffic flow variation over the week. Urban background sites revealed the
577 same pattern, excluding sites in Northern Ireland, where the concentration of BC was fairly constant
578 during the week, due to influences from sources other than vehicle emissions. BrC showed elevated
579 levels during weekends at all sites apart from rural sites as these sites are less affected by
580 anthropogenic emissions. As was the case for traffic-related pollutants, OC with its both primary
581 and secondary components decreased at weekends at kerbside and urban sites, whereas it was
582 constant at rural Harwell.

583

584 BrC revealed high levels at all study sites during winter (the heating season) and low levels in
585 summer. At urban background sites, BC showed the same seasonality as BrC, while rural sites
586 revealed no seasonal dependence as regional background concentrations are dominant. Primary
587 pollutants and SOC at North Kensington revealed elevated levels during the cold months, whereas
588 SOC was the only pollutant at Harwell which revealed seasonal dependence and was enhanced by
589 photochemistry in summer.

590

591 BC levels have dropped in the UK over the years 2009- 2017, the highest decrease in BC being at
592 Marylebone Road which gives strong evidence for the effectiveness of pollution abatement
593 strategies to reduce vehicle emissions, especially in London. On the other hand, BrC increased over
594 the study period at Marylebone Road. All urban background sites showed a downward trend in BrC
595 levels, but this change was not significant, except at Ballymena and Birmingham Tyburn, whereas
596 OC, POC and SOC decreased significantly at kerbside and rural sites, but the POC trend was not
597 significant.

598

599 South-easterly and easterly winds were the major wind directions which enhanced the
600 concentrations of pollutants at different sites. This emphasizes the importance of long-range
601 transport from Europe for primary and secondary pollutants levels in the UK, as well as being
602 associated with meteorological conditions which are not conducive to effective dispersion.

603

604 The regression analysis of BC and EC revealed that the aethalometer overestimates BC
605 concentrations, and that the mass absorption coefficient should be recalibrated if the data are to be
606 more reflective of EC concentrations.

607

608 **DATA AVAILABILITY**

609 Data supporting this publication are openly available from the UBIRA eData repository at
610 <https://doi.org/10.25500/edata.bham.00000516>

611

612 **ACKNOWLEDGEMENTS**

613 The authors acknowledge the Department for Environment, Food and Rural Affairs (DEFRA) and
614 uk-air.defra.gov.uk for providing the access to the air pollution monitoring network database.

615

616 **SUPPORTING INFORMATION**

617 Supporting Information provides further details of short and long-term temporal trends of
618 carbonaceous aerosols at all the study sites, together with polar plots of pollutant concentrations in
619 relation to wind speed and direction; in addition to the regression analysis of BC and EC; and the
620 estimation of $(OC/EC)_{min}$.

621

622 **CONFLICT OF INTERESTS**

623 The authors declare no competing financial interest.

624

625 **REFERENCES**

- 626
- 627 Ahmed, T., Dutkiewicz, V. A., Khan, A. J. and Husain, L., 2014. Long term trends in black carbon
628 concentrations in the northeastern United States. *Atmos. Res.* 137, 49-57.
- 629
- 630 Andreae, M. O. and Gelencsér, A., 2006. Black carbon or brown carbon? The nature of light-
631 absorbing carbonaceous aerosols. *Atmos. Chem. Phys.* 6, 3131-3148.
- 632
- 633 Agustine, I., Yulinawati, H., Suswanto, E. and Gunawan, D., 2017. Application of open air model
634 (R package) to analyze air pollution data. *Indones. J. Urban Environ. Technol.* 1, 94-108.
- 635
- 636 Ayers, G., 2001. Comment on regression analysis of air quality data. *Atmos. Environ.* 35, 2423-
637 2425.
- 638
- 639 Backman, J., Rizzo, L.V., Hakala, J., Nieminen, T., Manninen, H.E., Morais, F., Aalto, P. P.,
640 Siivola, E., Carbone, S., Hillamo, R. and Artaxo Netto, P. E., 2012. On the diurnal cycle of urban
641 aerosols, black carbon and the occurrence of new particle formation events in springtime São Paulo,
642 Brazil. *Appl. Radiat. Isot.* 12, 11733-11751.
- 643
- 644 Bahadur, R., Praveen, P. S., Xu, Y. and Ramanathan, V., 2012. Solar absorption by elemental and
645 brown carbon determined from spectral observations. *PNAS* 109, 17366-17371.
- 646
- 647 Beccaceci, S., Mustoe, C., Butterfield, D., Tompkins, J., Sarantaridis, D., Quincey, P., Brown, R.,
648 Green, D., Fuller, G., Tremper, A., Priestman, M., Font Font, A., Jones, A., 2013. Airborne
649 Particulate Concentrations and numbers in the United Kingdom (phase 3): Annual Report – 2012,
650 [https://uk-](https://uk-air.defra.gov.uk/assets/documents/reports/cat05/1312100920_Particles_Network_Annual_report_2012_AS_83.pdf)
651 [air.defra.gov.uk/assets/documents/reports/cat05/1312100920_Particles_Network_Annual_report_20](https://uk-air.defra.gov.uk/assets/documents/reports/cat05/1312100920_Particles_Network_Annual_report_2012_AS_83.pdf)
652 [12_AS_83.pdf](https://uk-air.defra.gov.uk/assets/documents/reports/cat05/1312100920_Particles_Network_Annual_report_2012_AS_83.pdf) [last accessed 28/05/2020].
- 653
- 654 Butterfield, D., Beccaceci, S., Quincey, P., Sweeney, B., Whiteside, K., Fuller, G., Green, D. and
655 Grieve, A., 2016. 2015 Annual Report for the UK Black Carbon Network, [https://uk-](https://uk-air.defra.gov.uk/assets/documents/reports/cat13/1611011539_2015_Black_Carbon_Network_Annual_Report_Final_18082016.pdf)
656 [air.defra.gov.uk/assets/documents/reports/cat13/1611011539_2015_Black_Carbon_Network_Annu](https://uk-air.defra.gov.uk/assets/documents/reports/cat13/1611011539_2015_Black_Carbon_Network_Annual_Report_Final_18082016.pdf)
657 [al_Report_Final_18082016.pdf](https://uk-air.defra.gov.uk/assets/documents/reports/cat13/1611011539_2015_Black_Carbon_Network_Annual_Report_Final_18082016.pdf) [last accessed 28/05/2020].
- 658
- 659 Butterfield, D., Beccaceci, S., Quincey, P., Sweeney, B., Whiteside, K., Fuller, G., Green, D. and
660 Grieve, A., 2013. 2012 Annual Report for the UK Black Carbon Network, [https://uk-](https://uk-air.defra.gov.uk/assets/documents/reports/cat13/1309060901_2012_BC_Network_Annual_Report-Final.pdf)
661 [air.defra.gov.uk/assets/documents/reports/cat13/1309060901_2012_BC_Network_Annual_Report-](https://uk-air.defra.gov.uk/assets/documents/reports/cat13/1309060901_2012_BC_Network_Annual_Report-Final.pdf)
662 [Final.pdf](https://uk-air.defra.gov.uk/assets/documents/reports/cat13/1309060901_2012_BC_Network_Annual_Report-Final.pdf) [last accessed 28/05/2020].
- 663
- 664 Carslaw, D. C., 2015. The openair manual — open-source tools for analysing. London, Manual for
665 version 1.1-4, King’s College, London.
- 666
- 667 Carslaw, D.C., Ropkins, K., 2012. openair - an R package for air quality data analysis, *Environ.*
668 *Model Softw.* 27-28, 52-61.
- 669
- 670 Cavalli, F., Alastuey, A., Areskoug, H., Ceburnis, D., Čech, J., Genberg, J., Harrison, R. M.,
671 Jaffrezo, J. L., Kiss, G., Laj, P. and Mihalopoulos, N., 2016. A European aerosol phenomenology-4:
672 Harmonized concentrations of carbonaceous aerosol at 10 regional background sites across Europe.
673 *Atmos. Environ.* 144, 133-145.

674 Chakrabarty, R. K., Moosmüller, H., Chen, L.W., Lewis, K., Arnott, W. P., Mazzoleni, C., Dubey,
675 M. K., Wold, C. E., Hao, W. M. and Kreidenweis, S. M., 2010. Brown carbon in tar balls from
676 smoldering biomass combustion. *Atmos. Chem. Phys.* 10, 6363-6370.
677

678 Chang, Y., Deng, C., Cao, F., Cao, C., Zou, Z., Liu, S., Lee, X., Li, J., Zhang, G. and Zhang, Y.,
679 2017. Assessment of carbonaceous aerosols in Shanghai, China-Part 1: Long-term evolution,
680 seasonal variations, and meteorological effects. *Atmos. Chem. Phys.* 17, 9945–9964.
681

682 Charron, A., Degrendele, C., Laongsri, B. and Harrison, R. M., 2013. Receptor modelling of
683 secondary and carbonaceous particulate matter at a southern UK site. *Atmos. Chem. Phys.* 13,
684 1879-1894.
685

686 Chen, L. W., Chow, J. C., Watson, J. G. and Schichtel, B. A., 2012. Consistency of long-term
687 elemental carbon trends from thermal and optical measurements in the IMPROVE network. *Atmos.*
688 *Meas. Tech.* 5, 2329-2338.
689

690 Chen, Y. and Bond, T.C., 2010. Light absorption by organic carbon from wood combustion. *Atmos.*
691 *Chem. Phys.* 10, 1773–1787.
692

693 Contini, D., Vecchi, R. and Viana, M., 2018, Carbonaceous aerosols in the atmosphere. *Atmosphere*
694 9, 181, doi:10.3390/atmos9050181.
695

696 DEFRA, 2019. UK Air Information Resource, <https://uk-air.defra.gov.uk/> [last accessed 15 January
697 2019].

698 Font, A., Guiseppin, L., Blangiardo, M., Ghersi, V. and Fuller, G.W., 2019. A tale of two cities: is
699 air pollution improving in Paris and London? *Environ. Pollut.* 249, 1-12.
700

701 Garrett, R. G., 2018. Package ‘rgr’, Applied Geochemistry EDA, [https://cran.r-](https://cran.r-project.org/web/packages/rgr/rgr.pdf)
702 [project.org/web/packages/rgr/rgr.pdf](https://cran.r-project.org/web/packages/rgr/rgr.pdf) [last accessed 25 6 2019].
703

704 Hallquist, M., Wenger, J. C., Baltensperger, U., Rudich, Y., Simpson, D., Claeys, M., Dommen, J.,
705 Donahue, N. M., George, C., Goldstein, A. H. and Hamilton, J.F., 2009. The formation, properties
706 and impact of secondary organic aerosol: current and emerging issues. *Atmos. Chem. Phys.* 9,
707 5155-5236.
708

709 Hand, J. L., Schichtel, B. A., Malm, W. C. and Frank, N. H., 2013. Spatial and temporal trends in
710 PM_{2.5} organic and elemental carbon across the United States. *Adv. Meteorol.* 367674,
711 <http://dx.doi.org/10.1155/2013/367674>.
712

713 Harrison, R. M., Beddows, D. C., Jones, A. M., Calvo, A., Alves, C. and Pio, C., 2013. An
714 evaluation of some issues regarding the use of aethalometers to measure woodsmoke
715 concentrations. *Atmos. Environ.* 80, 540-548.
716

717 Harrison, R.M. and Yin, J., 2008. Sources and processes affecting carbonaceous aerosol in central
718 England. *Atmos. Environ.* 42, 1413-1423.
719

720 Jones, A.M. and Harrison, R.M., 2005. Interpretation of particulate elemental and organic carbon
721 concentrations at rural, urban and kerbside sites. *Atmos. Environ.* 39, 7114-7126.
722

723 Kucbel, M., Corsaro, A., Švédová, B., Raclavská, H., Raclavský, K. and Juchelková, D., 2017.
724 Temporal and seasonal variations of black carbon in a highly polluted European city:
725 Apportionment of potential sources and the effect of meteorological conditions. *J. Environ.*
726 *Manage.* 203, 1178-1189.
727

728 Kutzner, R. D., von Schneidmesser, E., Kuik, F., Quedenau, J., Weatherhead, E.C. and Schmale,
729 J., 2018. Long-term monitoring of black carbon across Germany. *Atmos. Environ.* 185, 41-52.
730

731 Lack, D. A., Moosmüller, H., McMeeking, G. R., Chakrabarty, R. K. and Baumgardner, D., 2014.
732 Characterizing elemental, equivalent black, and refractory black carbon aerosol particles: a review
733 of techniques, their limitations and uncertainties. *Anal. Bioanal. Chem.* 406, 99-122.
734

735 Lin, P., Hu, M., Deng, Z., Slanina, J., Han, S., Kondo, Y., Takegawa, N., Miyazaki, Y., Zhao, Y.
736 and Sugimoto, N., 2009. Seasonal and diurnal variations of organic carbon in PM_{2.5} in Beijing and
737 the estimation of secondary organic carbon. *J. Geophys. Res. Atmos.* 114, D00G11,
738 doi:10.1029/2008JD010902.
739

740 Liu, J., Bergin, M., Guo, H., King, L., Kotra, N., Edgerton, E. and Weber, R.J., 2013. Size-resolved
741 measurements of brown carbon in water and methanol extracts and estimates of their contribution to
742 ambient fine-particle light absorption. *Atmos. Chem. Phys.* 13, 12389–12404.
743

744 Lukács, H., Gelencsér, A., Hammer, S., Puxbaum, H., Pio, C., Legrand, M., Kasper-Giebl, A.,
745 Handler, M., Limbeck, A., Simpson, D. and Preunkert, S., 2007. Seasonal trends and possible
746 sources of brown carbon based on 2-year aerosol measurements at six sites in Europe. *J. Geophys.*
747 *Res. Atmos.* 112, D23S18, doi:10.1029/2006JD008151.
748

749 Luoma, K., Niemi, J. V., Helin, A., Aurela, M., Timonen, H., Virkkula, A., Rönkkö, T., Kousa, A.,
750 Fung, P. L., Hussein, T., and Petäjä, T., 2020. Spatiotemporal variation and trends of equivalent
751 black carbon in the Helsinki metropolitan area in Finland. *Atmos. Chem. Phys. Discuss.*
752 <https://doi.org/10.5194/acp-2020-201>.
753

754 Mbengue, S., Fusek, M., Schwarz, J., Vodička, P., Šmejkalová, A. H. and Holoubek, I., 2018. Four
755 years of highly time resolved measurements of elemental and organic carbon at a rural background
756 site in Central Europe. *Atmos. Environ.* 182, 335-346.
757

758 Merico, E., Cesari, D., Dinoi, A., Gambaro, A., Barbaro, E., Guascito, M.R., Giannossa,
759 L.C., Mangone, A., Contini, D., 2019. Inter-comparison of carbon content in PM₁₀ and
760 PM_{2.5} measured with two thermo-optical protocols on samples collected in a Mediterranean
761 site. *Environ. Sci Pollut. Res.* 26, 29334-29350.
762

763 Nataraj, P., Fauzie, A.K., Rani, P.S. and Venkataramana, G.V., 2020. Dispersion of Nitrogen
764 Dioxide and Particulate Matter Concentrations in Street Canyons and Open Landscape in Urban
765 Mysore. *Humanities* 7, 36-43.
766

767 Nataraj, P., Fauzie, A.K., Rani, P.S. and Venkataramana, G.V., 2020. Dispersion of Nitrogen
768 Dioxide and Particulate Matter Concentrations in Street Canyons and Open Landscape in Urban
769 Mysore. *Humanities* 7, 36-43
770

771 National Physical Laboratory, 2016a, Airborne Particulate Concentrations and Numbers in the
772 United Kingdom (phase 3) Annual report 2015, <https://uk->

773 air.defra.gov.uk/assets/documents/reports/cat09/1807161507_Particles_Network_Annual_Report_2
774 015.pdf
775
776 National Physical Laboratory, 2016b. 2015 Annual Report for the UK Black Carbon Network,
777 <http://eprintspublications.npl.co.uk/7276/1/ENV7.pdf>
778
779 Petzold, A., Ogren, J. A., Fiebig, M., Laj, P., Li, S. M., Baltensperger, U., Holzer-Popp, T., Kinne,
780 S., Pappalardo, G., Sugimoto, N. and Wehrli, C., 2013. Recommendations for reporting "black
781 carbon" measurements. *Atmos. Chem. Phys.* 13, 8365-8379.
782
783 Pio, C., Cerqueira, M., Harrison, R.M., Nunes, T., Mirante, F., Alves, C., Oliveira, C., de la Campa,
784 A.S., Artíñano, B. and Matos, M., 2011. OC/EC ratio observations in Europe: Re-thinking the
785 approach for apportionment between primary and secondary organic carbon. *Atmos. Environ.* 45,
786 6121-6132.
787
788 Querol, X., Alastuey, A., Viana, M., Moreno, T., Reche, C., Minguillón, M.C., Ripoll, A., Pandolfi,
789 M., Amato, F., Karanasiou, A. and Pérez, N., 2013. Variability of carbonaceous aerosols in remote,
790 rural, urban and industrial environments in Spain: implications for air quality policy. *Atmos. Chem.*
791 *Phys.* 13, 6185-6206.
792
793 Ramanathan, V. and Carmichael, G., 2008. Global and regional climate changes due to black
794 carbon. *Nat. Geosci.* 1, 221-227.
795
796 Reche, C., Querol, X., Alastuey, A., Viana, M., Pey, J., Moreno, T., Rodríguez, S., González, Y.,
797 Fernández-Camacho, R., de la Rosa, J., Dall'Osto, M., Prévôt, A. S. H., Hueglin, C., Harrison, R.
798 M. and Quincey, P., 2011. New considerations for PM, black carbon and particle number
799 concentration for air quality monitoring across different European cities. *Atmos. Chem. Phys.* 11,
800 6207-6227.
801
802 Richmond B, Misra A, Broomfield M, Brown P, Karagianni E, Murrells T, Pang Y, Passant N,
803 Pearson B, Stewart R, Thistlethwaite G, Wakeling D, Walker C, Wiltshire J, Hobson M, Gibbs M,
804 Misselbrook T, Dragosits U, Tomlinson S, 2020. Report: UK Informative Inventory Report (1990
805 to 2018,UK-Air, [https://uk-](https://uk-air.defra.gov.uk/assets/documents/reports/cat07/2003131327_GB_IIR_2020_v1.0.pdf)
806 [air.defra.gov.uk/assets/documents/reports/cat07/2003131327_GB_IIR_2020_v1.0.pdf](https://uk-air.defra.gov.uk/assets/documents/reports/cat07/2003131327_GB_IIR_2020_v1.0.pdf)
807
808 Sahu, L. K., Kondo, Y., Miyazaki, Y., Pongkiatkul, P. and Kim Oanh, N. T., 2011. Seasonal and
809 diurnal variations of black carbon and organic carbon aerosols in Bangkok. *J. Geophys. Res.*
810 *Atmos.* 116, D15302, <https://doi.org/10.1029/2010JD015563>.
811
812 Sandrini, S., Fuzzi, S., Piazzalunga, A., Prati, P., Bonasoni, P., Cavalli, F., Bove, M. C., Calvello,
813 M., Cappelletti, D., Colombi, C. and Contini, D., 2014. Spatial and seasonal variability of
814 carbonaceous aerosol across Italy. *Atmos. Environ.* 99, 587-598.
815
816 Sharma, S., Leitch, W. R., Huang, L., Veber, D., Kolonjari, F., Zhang, W., Hanna, S. J., Bertram,
817 A. K. and Ogren, J.A., 2017. An evaluation of three methods for measuring black carbon in Alert,
818 Canada. *Atmos. Chem. Phys.* 17, 15225-15243.
819
820 Singh, V., Ravindra, K., Sahu, L. and Sokhi, R., 2018. Trends of atmospheric black carbon
821 concentration over the United Kingdom. *Atmos. Environ.* 178, 48-157.
822

823 Sommer, E., Wonaschütz, A., Haller, T., Kasper, J. and Hitzenberger, R., 2019. Past and present
824 trends of black and brown carbon concentrations in the Vienna urban aerosol. *Geophys. Res. Abstr.*
825 21, EGU2019-8866.

826

827 Sun, L., Birmili, W., Hermann, M., Tuch, T., Weinhold, K., Merkel, M., Rasch, F., Müller, T.,
828 Schladitz, A., Bastian, S., Löschau, G., Cyrus, J., Gu, J., Flentje, H., Briel, B., Gunter, C.,
829 Kaminski, H., Ries, L., Sohmer, R., Gerwig, H., Wirtz, K., Asbach, C., Meinhardt, F., Schwerin, A.,
830 Bath, O., Ma, N., and Wiedensohler, A., 2020. Decreasing trends of particle number and black
831 carbon mass concentrations at 16 observational sites in Germany from 2009 to 2018. *Atmos. Chem.*
832 *Phys.* 20, 7049–7068.

833

834 Titos, G., Del Águila, A., Cazorla, A., Lyamani, H., Casquero-Vera, J. A., Colombi, C., Cuccia, E.,
835 Gianelle, V., Močnik, G., Alastuey, A. and Olmo, F. J., 2017. Spatial and temporal variability of
836 carbonaceous aerosols: assessing the impact of biomass burning in the urban environment. *Sci. Tot.*
837 *Environ.* 578, 613-625.

838

839 Tiwari, S., Srivastava, A.K., Bisht, D. S., Parmita, P., Srivastava, M. K. and Attri, S. D., 2013.
840 Diurnal and seasonal variations of black carbon and PM_{2.5} over New Delhi, India: influence of
841 meteorology. *Atmos. Res.* 125, 50-62.

842

843 Viana, M., Reche, C., Amato, F., Alastuey, A., Querol, X., Moreno, T., Lucarelli, F., Nava, S.,
844 Calzolari, G., Chiari, M. and Rico, M., 2013. Evidence of biomass burning aerosols in the Barcelona
845 urban environment during winter time. *Atmos. Environ.* 72, 81-88.

846

847 Wang, R., Tao, S., Shen, H., Huang, Y., Chen, H., Balkanski, Y., Boucher, O., Ciais, P., Shen, G.,
848 Li, W. and Zhang, Y., 2014. Trend in global black carbon emissions from 1960 to 2007. *Environ.*
849 *Sci. Technol.* 48, 6780-6787.

850

851 Weimer, S., Mohr, C., Richter, R., Keller, J., Mohr, M., Prevot, A.S.H. and Baltensperger, U., 2009.
852 Mobile measurements of aerosol number and volume size distributions in an Alpine valley:
853 Influence of traffic versus wood burning. *Atmos. Environ.* 43, 624-630.

854

855 WHO, 2012. Health Effects of Black Carbon,
856 http://www.euro.who.int/__data/assets/pdf_file/0004/162535/e96541.pdf?ua=1 [last accessed
857 27/05/2020].

858

859 Yin, J., Harrison, R. M., Chen, Q., Rutter, A. and Schauer, J. J., 2010. Source apportionment of fine
860 particles at urban background and rural sites in the UK atmosphere. *Atmos. Environ.* 44, 841-851.

861

862 Yin, J. and Harrison, R.M., 2008. Pragmatic mass closure study for PM_{1.0}, PM_{2.5} and PM₁₀ at
863 roadside, urban background and rural sites. *Atmos. Environ.* 42, 980-988.

864

865 Zheng, H., Kong, S., Zheng, M., Yan, Y., Yao, L., Zheng, S., Yan, Q., Wu, J., Cheng, Y., Chen, N.
866 and Bai, Y., 2020. A 5.5-year observations of black carbon aerosol at a megacity in Central China:
867 Levels, sources, and variation trends. *Atmos. Environ.* 232, 117581.

868

869 Zotter, P., Herich, H., Gysel, M., El-Haddad, I., Zhang, Y., Močnik, G., Hüglin, C., Baltensperger,
870 U., Szidat, S. and Prévôt, A. S., 2017. Evaluation of the absorption Ångström exponents for traffic
871 and wood burning in the Aethalometer-based source apportionment using radiocarbon
872 measurements of ambient aerosol. *Atmos. Chem. Phys.* 17, 4229-4249.

873 **LIST OF TABLE LEGENDS**

874

875 **Table 1:** Study sites classification, government region and monitoring period.

876

877 **Table 2:** The annual $(OC/EC)_{min}$ At Marylebone Road, North Kensington and Harwell Over
878 the Study Period.

879

880

881 **LIST OF FIGURE LEGENDS**

882

883 **Figure 1:** Map of air sampling study sites.

884

885 **Figure 2:** The diurnal and day of the week variation in BC in Marylebone Road.

886

887 **Figure 3:** The monthly variation in BC and BrC in Marylebone Road.

888

889 **Figure 4:** Trends in BC and BrC based on monthly mean concentrations at Marylebone Road.
890 (The solid red line represents the mean trend and the dashed lines represent the 95%
891 confidence interval. The trend and confidence interval are shown at the top as $\mu\text{g m}^{-3}$ /
892 year. The * * * show that the trend is significant at the $p < 0.001$ level).

893

894 **Figure 5:** Polar plot of mean BC and BrC concentrations at Marylebone Road over the period
895 2009-2017.

896

897 **Figure 6:** Polar plot of mean BC and BrC concentrations at Detling over the period 2013-2017.

898

899 **Figure 7:** Regression of EC and BC at Marylebone Road, North Kensington and Harwell over
900 the study period. (The black dashed line represents 1:1. while the red dashed line
901 represents the regression line, N is the number of measurements and Fit represents
902 R^2).

903

904 **Table 1:** Study sites classification, government region and monitoring period.

Site Name	Classification	Government Region	Monitoring Period
London N. Kensington	Urban Background	Greater London	2009-2017
London Marylebone Road	Urban Traffic	Greater London	2009-2017
Birmingham Tyburn	Urban Background	West Midlands	2009-2016
Auchencorth Moss	Rural Background	Central Scotland	2012-2017
Belfast Centre	Urban Background	Northern Ireland	2009-2017
Strabane 2	Suburban Background	Northern Ireland	2009-2017
Ballymena Ballykeel	Urban Background	Northern Ireland	2013-2017
Kilmakee Leisure Centre	Urban Background	Northern Ireland	2013-2017
Cardiff	Urban Background	South Wales	2009-2013
Detling	Rural Background	South East	2013-2017
Harwell	Rural Background	South East	2009-2015

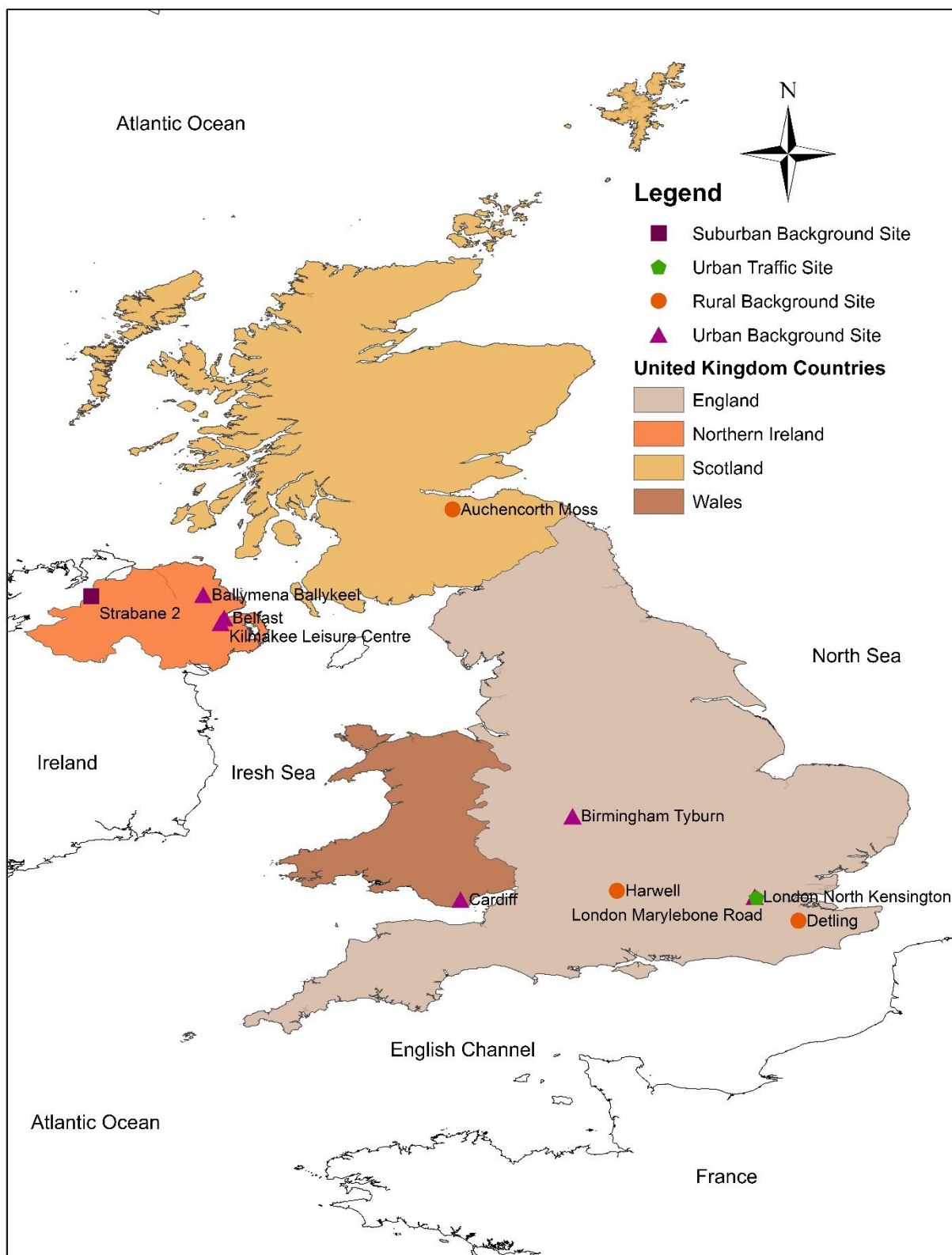
905
906

907 **Table 2:** The annual $(OC/EC)_{min}$ At Marylebone Road, North Kensington and Harwell Over the
908 Study Period.

909

Year	Marylebone Road	North Kensington	Harwell
2010	0.50	1.25	2.00
2011	0.41	1.60	2.60
2012	0.36	1.30	3.00
2013	0.51	1.60	3.20
2014	0.51	2.00	2.60
2015	0.68	2.10	2.50
2016	0.60	1.10	
2017	0.83	1.60	

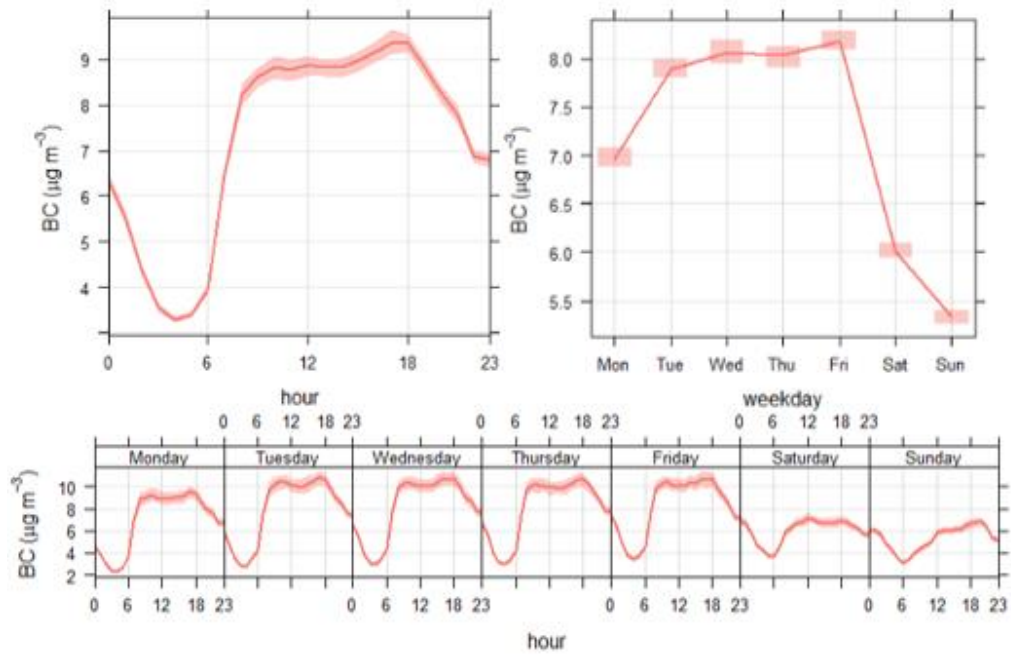
910



911
 912 **Figure 1:** Map of air sampling study sites.

913

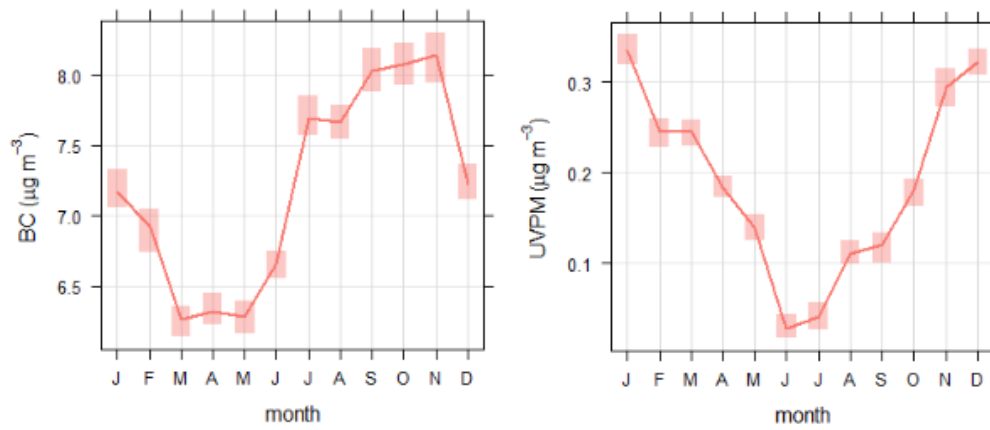
914



915
916
917
918

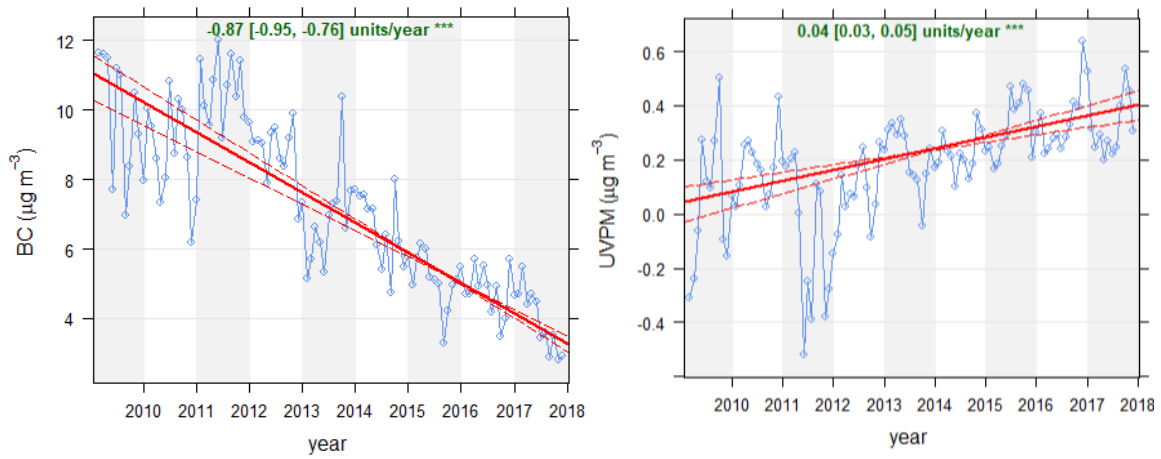
Figure 2: The diurnal and day of the week variation in BC in Marylebone Road.

919
920



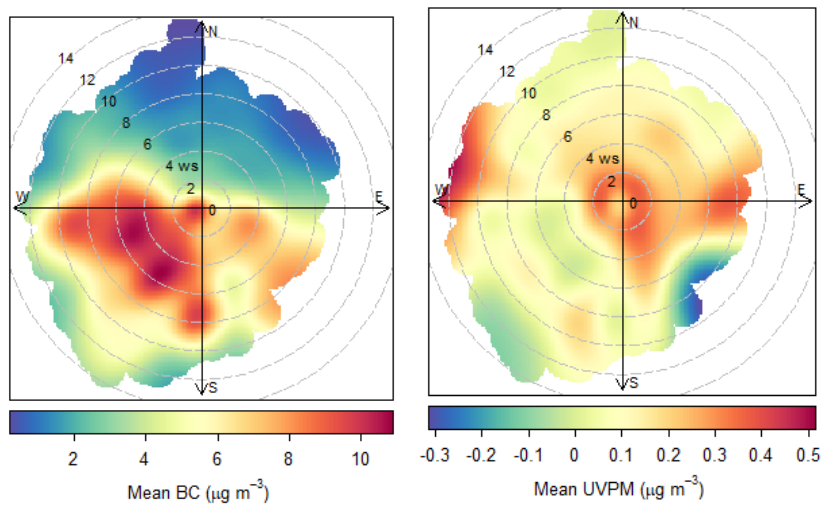
921
922
923
924
925

Figure 3: The monthly variation in BC and BrC in Marylebone Road.



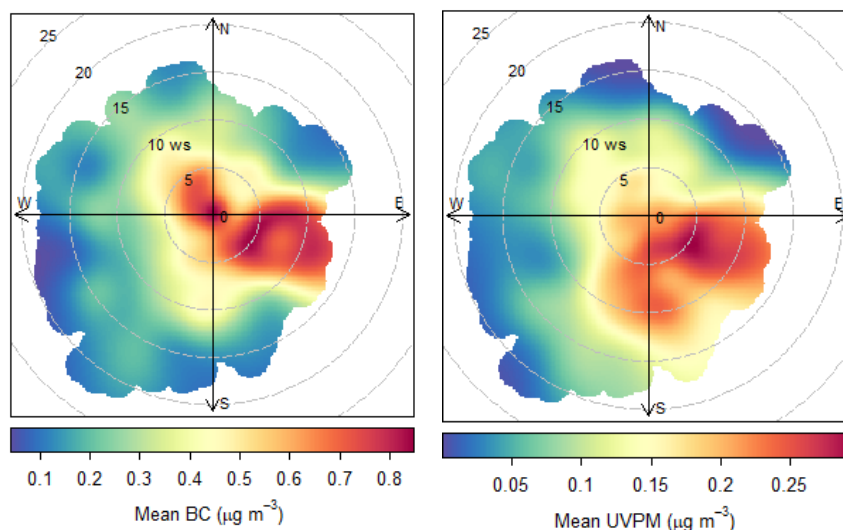
926
927
928
929
930
931
932
933
934

Figure 4: Trends in BC and BrC based on monthly mean concentrations at Marylebone Road. (The solid red line represents the mean trend and the dashed lines represent the 95% confidence interval. The trend and confidence interval are shown at the top as $\mu\text{g m}^{-3}/\text{year}$. The * * * show that the trend is significant at the $p < 0.001$ level).



935
936
937
938
939
940

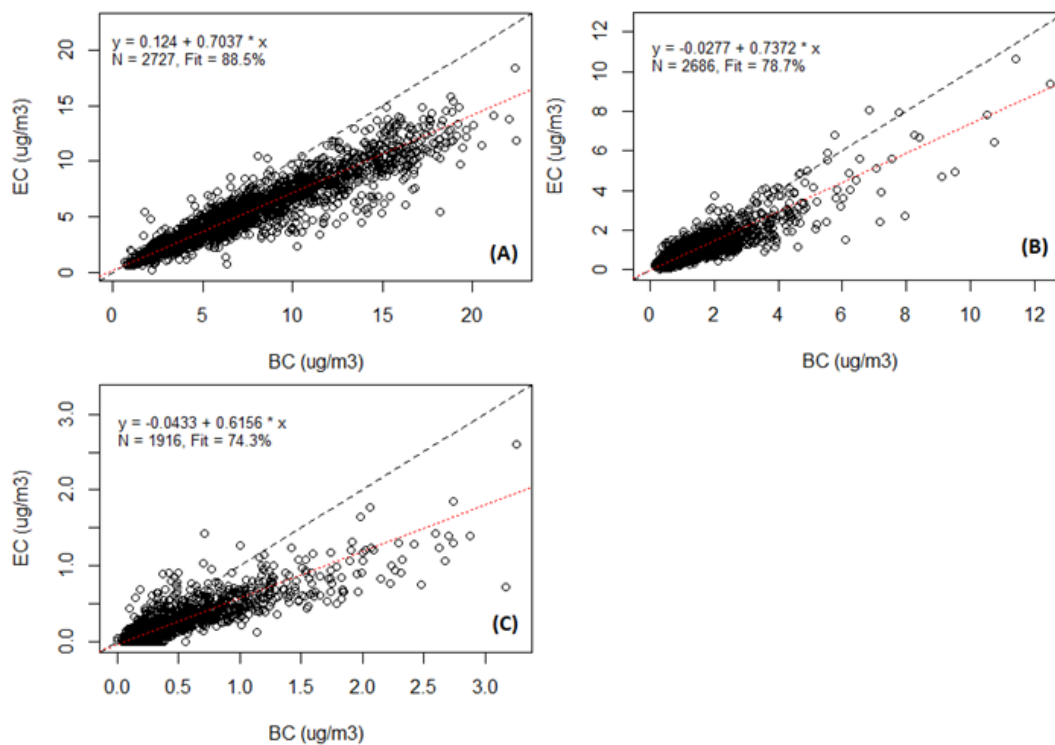
Figure 5: Polar plot of mean BC and BrC concentrations at Marylebone Road over the period 2009-2017.



941
942

943 **Figure 6:** Polar plot of mean BC and BrC concentrations at Detling over the period 2013-2017.

944



945
946
947
948
949
950

Figure 7: Regression of EC and BC at Marylebone Road, North Kensington and Harwell over the study period. (The black dashed line represents 1:1, while the red dashed line represents the regression line, N is the number of measurements and Fit represents R^2).